Theor Chem Acc (2011) 130:419–427
DOI 10.1007/s00214-011-1009-6

REGULAR ARTICLE

A benchmark quantum chemical study of the stacking interaction between larger polycondensed aromatic hydrocarbons

Tomasz Janowski · Peter Pulay

Received: 24 May 2011 / Accepted: 18 July 2011 / Published online: 6 August 2011
© Springer-Verlag 2011

Abstract Large-scale electronic structure calculations were performed for the interaction energy between coronene, $C_{24}H_{12}$ with circumcoronene, $C_{54}H_{18}$, and between two circumcoronene molecules, in order to get a picture of the interaction between larger graphene sheets. Most calculations were performed at the SCS-MP2 level but we have corrected them for higher-order correlation effects using a calculation on the coronene-circumcoronene system at the quadratic CI, QCISD(T) level. Our best estimate for the interaction energy between coronene and circumcoronene is 32.1 kcal/mol. We estimate the binding of coronene on a graphite surface to be 37.4 or 1.56 kcal/mol per carbon atom (67.5 meV/C atom). This is also our estimate for the exfoliation energy of graphite. It is higher than most previous theoretical estimates. The SCS-MP2 method which reproduces the CCSD(T) and QCISD(T) values very well for smaller aromatic hydrocarbons, e.g., for the benzene dimer, increasingly overestimates dispersion as the bandgap (the HOMO-LUMO separation) decreases. The barrier to the sliding motion of coronene on circumcoronene is 0.45 kcal/mol, and for two circumcoronene molecules 1.85 kcal/mol (0.018 and 0.034 kcal/mol per C atom, respectively). This means that larger graphenes cannot easily glide over each other.

Keywords Dispersion · pi–pi interactions · SCS-MP2 · Coupled cluster and quadratic configuration interaction · Graphene · Perturbative triples correction · Coronene · Circumcoronene · Exfoliation energy of graphite · Sliding of graphene sheets over each other · Electrostatic models of dispersion

1 Introduction

Aromatic carbon sheets are important for several reasons. Large conjugated systems: graphite, graphene sheets, carbon nanotubes, and fullerenes have already important applications and are being intensely investigated for future roles in nanotechnology, in electronics and as structural materials. Polycondensed aromatic hydrocarbons are ubiquitous environmental contaminants and, according to spectroscopic evidence, are present in interstellar material. Stacking interactions between π systems are important in both biochemistry and materials science. They are significant for protein conformation and are one of the main factors stabilizing nucleic acids [1–5]. The macroscopic properties of carbon-based materials are largely determined by π–π stacking interactions. Similar interactions are also present in porphyrins which are electronically similar to coronene, and in some inorganic systems [6, 7]. A number of ab initio studies [8–21] have addressed the interaction between π systems.

Most of these studies use the supermolecule approach, i.e., calculate the difference between the energy of the dimer and the energy of the monomers. However, the quantitative description of intermolecular energies in this approach turned out to be a surprisingly demanding task for

Dedicated to Professor Shigeru Nagase on the occasion of his 65th birthday. Published as part of the Nagase Festschrift Issue, and in recognition of his pioneering contributions to molecular and electronic structure theory, particularly in the field of silicon and fullerene chemistry.

T. Janowski · P. Pulay (✉)
Department of Chemistry and Biochemistry,
University of Arkansas, Fayetteville, AR 72701, USA
e-mail: pulay@uark.edu

T. Janowski
e-mail: janowski@uark.edu

two reasons. First, π interactions are dominated by dispersion forces. Dispersion is a pure correlation effect and is not accounted for at the Hartree–Fock level. Local and semilocal density functional theory provides a good description of short-range electron correlation but does not account for long-range correlation [22]. Some exchange–correlation functionals, including the simplest functional, Dirac-Slater exchange [23] and the local density approximation [24] yield a deep minimum at the interatomic potential at approximately the van der Waals distance, e.g., for the argon dimer [25]. However, the origin of this term is exchange, not correlation, and therefore it cannot have the required R^{-6} leading term of the dispersion interaction.

The simplest method to describe dispersion *for the right reason* is second-order many-body perturbation theory. With the Møller-Plesset partitioning, this is widely used as MP2 and is quite efficient. Unfortunately, MP2 strongly overestimates dispersion in π systems [8, 13]. The reason for this is most likely the neglect of interaction between correlated pairs which is largely repulsive. In addition, at typical van der Waals distances there is cancelation between dispersion attraction and Pauli repulsion, resulting in error amplification. An added difficulty is that the basis set superposition error (BSSE) for small- and moderate-sized basis sets are of the same order of magnitude as dispersion energies and the binding energy must be corrected for BSSE. Thus, the only direct way of obtaining benchmark quality π stacking interactions is to carry out high-level ab initio calculations with appropriate basis sets.

Because of the importance and the difficulty of the problem, a number of alternative, less costly approaches have been developed for intermolecular interactions. However, none of them can serve as a benchmark. Some are restricted to large or asymptotic distances. Other more recent methods do not follow rigorously from first principles, and contain empirical or intuitive elements which require calibration. The main purpose of the present paper is to report benchmark quality dispersion energies for the interaction between large aromatic π systems which were inaccessible for accurate calculations in the past, for the purpose of testing and calibrating these methods.

Below, we will discuss briefly the main alternative approaches. The dispersion interaction of two separated molecules can be readily calculated from frequency-dependent polarizabilities of the monomers at imaginary frequencies. However, this approach, without empirical damping, is limited to the asymptotic region where the monomer electron clouds do not overlap. The most rigorous alternative method is symmetry adapted perturbation theory [26]. An important advantage of this method is that the interaction energy can be decomposed to physically meaningful components. However, practical versions of SAPT are not free of empirical parameters, SAPT is not as generally applicable as the supermolecule treatment [27], and fully ab initio versions of it are also computationally expensive.

The overestimation of the dispersion component of MP2 can be improved considerably by empirical scaling of the separate spin contributions, as done in the SCS-MP2 and SOS-MP2 methods [28, 29], or by mixing MP2 and MP3 [30]. These methods perform quite well, although they do not appear to have a solid theoretical foundation. The SCS-MP2 and SOS-MP2 methods also underestimate dispersion (the C_6 coefficient) at asymptotic distances where the parallel and opposite spin components become equal.

An inexpensive way of accounting for dispersion is to augment local DFT with atom-based empirical dispersion terms, usually just the dominant R^{-6} terms, in the spirit of molecular mechanics [31]. These methods are expected to perform well for well-localized systems. However, their performance for large delocalized systems like larger graphitic sheets is uncertain at best. The present results may be used to refine them. The coefficients for the dispersion correction can be calculated non-empirically. Sato and Nakai [32] evaluate them from a non-empirical approximation to the local dynamic response function in DFT. In a similar approach, Adamovic and Gordon [33] evaluate dynamical polarizabilities at imaginary frequencies by the Coupled-Perturbed Hartree–Fock method and decompose them in localized contributions.

It can be proved rigorously that local and semilocal density functional theory (including functionals that include the kinetic energy density) is unable to describe genuine dispersion [21]. Nevertheless, the exchange energy in some DFT versions (for instance in the simple Dirac-Slater exchange [23]) is attractive at intermediate distance corresponding roughly to the van der Waals distance. Recent highly parametrized exchange–correlation functionals, in particular Truhlar's 2006 functionals [34–36] are promising candidates for describing intermolecular interactions in the van der Waals region, even though it appears that they accomplish this through the exchange, and therefore must fail in the asymptotical region. In the absence of accurate comparison data, the validity of these functionals for highly polarizable systems like large aromatic hydrocarbons has not been ascertained. Another approach is to modify the pseudopotentials commonly used to replace the atomic cores in DFT to simulate the dispersion interactions [37, 38]. These methods require calibration, for instance the pseudopotentials of Ref. [37] were fitted to MP2 calculations.

A method with a solid theoretical foundation is the van der Waals density functional of Langreth et al. [39, 40]. This method is non-local and requires double numerical integration with the concomitant computational cost. The functional, while physically plausible, is approximate and

therefore its results must be compared with definitive data. It has been used as the long-range component in Hirao's method [41].

A combination of methods has been proposed by Ángyán et al. [42], using local density functional theory for short range, and Hartree–Fock and MP2 theories for long range. Becke and Johnson [43] have developed a highly intuitive method that derives the dispersion from the electrostatic interaction of exchanges holes. This method also uses an empirical parameter, and, although it is based on an appealing physical picture, it does not appear to be derivable rigorously from the Schrödinger equation.

Given the inaccuracy of MP2 theory, and the fact that methods with scaling higher than $O(N^7)$ are still computationally unfeasible for the large molecules in this study, the only accurate and practical methods appropriate to stacking interactions between π systems are variants of singles and doubles coupled cluster (CC) theory (CCSD or QCISD) with perturbative triples corrections (see [44] for a review). Local correlation methods [45, 46] have much lower scaling but their applicability to these highly delocalized systems is not yet clear. The coupled electron pair approximation (CEPA/1) in conjunction with local pair (or pseudo) natural orbitals has been shown recently to yield excellent binding energies for weakly bound complexes, including difficult cases like the benzene dimer [47] at modest computational cost. However, since it does not contain explicit triple substitutions which are very important for π–π interactions, the good agreement for LPNO-CEPA must be semiempirical to a certain extent, relying on the slight overestimation of the doubles contribution which mimics the missing triples. This leaves coupled cluster with triples corrections as the only reference quality method. Since its introduction [48] several variants of the perturbative triples correction have been proposed, the most popular being CCSD(T) [49], considered by many the "gold standard" of quantum chemistry. However, its steep $O(N^7)$ scaling, with the system size N prevented its application to larger π stacked dimers until very recently. Improved computer performance and advances in formulating and parallelizing the CCSD(T) equations enabled the conclusive determination of the benzene dimer potential [13–19, 21]. Larger systems with π interactions have been still beyond the reach of CC methods with large basis sets. We have recently completed the development of an efficient parallel CCSD(T)/QCISD(T) program that is capable of handling large molecules and basis sets on medium-sized computer clusters [50, 51]. The techniques employed in this program are described in Ref. [51]. CCSD(T), in spite of its excellent performance for dynamical correlation, breaks down in the presence of non-dynamical correlation, i.e., when the HOMO-LUMO energy gap becomes too small, because of its perturbative triples component. An infinite graphite sheet is a semimetal with zero bandgap at one point in the Brillouin zone, and therefore CCSD(T) will break down. However, for the systems treated here, the HOMO-LUMO gap is sufficiently large (>0.1 E_h) and CCSD(T) is expected to be reliable.

The work described in this paper is an extension of our earlier work on the coronene dimer [52]. Its main purpose is to generate benchmark data on π–π dispersion interactions for larger systems, compare the results with less expensive alternatives like SCS-MP2[28], parametrize the results, and extrapolate them to infinite graphene sheets.

2 Computational details

The highest level calculations were carried out at the QCISD(T) level. The reason for choosing the QCISD [53] over the more popular CCSD(T) is that it does not require the recomputation of the AO integrals in every cycle and is thus more efficient for our integral-direct program [50, 51]. The difference in the interaction energy provided by these two methods is negligible for the benzene dimer [21] and corannulene dimer [54].

All calculations were performed using the PQS program package [55]. The coupled cluster module in PQS allows large calculations or modest size parallel computers. While massive parallelism is the current center of attention, it is still quite difficult to allocate routinely more than a few hundred CPU cores at most computer centers, and therefore it is important to be able to handle large calculations on relatively small computer clusters. By using local disk storage, the PQS code can carry out large calculations on modest parallel clusters. The geometries of the monomers were optimized at the B3LYP/aug-cc-pVTZ level and were not reoptimized. All data were corrected for basis set superposition error by the Boys-Bernardi counterpoise correction.

A recurring problem in ab initio calculations with large atomic orbital (AO) basis sets is the overcompleteness problem. For large systems with diffuse basis sets, the AO basis becomes nearly linearly dependent. This is most prominent in 3-dimensional systems but 2-dimensional systems are also strongly affected; even linear chains show this behavior. The consequences are that the atomic orbital coefficients can become large, leading to large canceling contributions in the integrals over molecular orbitals, and strongly degrading the numerical precision of the results, to the point that the results become meaningless. In our opinion, this problem has not been sufficiently addressed in the current literature. As in our earlier work [52], we have used aDZ and aTZ basis sets which are applicable for alternant hydrocarbons. Recall that in alternant hydrocarbons, the carbon atoms can be assigned to two sets, none of

which contains atoms directly bonded to each other. In the aDZ and aTZ basis sets, the aug-cc-pVXZ basis set is used for the carbon atoms of one of these sets; the remaining atoms (including hydrogens) were assigned non-augmented cc-pVXZ basis. The validity of this construction was tested in Ref. 52. Omitting the augmentation functions in the aug-cc-pVDZ basis on every second C atom diminishes the calculated SCS-MP2 binding energy in the parallel displaced coronene dimer by 2.6% [52]. The error is larger (up to about 5%) in the benzene dimer, precisely because the basis set is not yet severely linearly dependent in this small system. However, the truncation effect is much smaller at the TZ level and negligible at QZ level (for the benzene dimer, the numbers are 1.3 and 0.5%, respectively). Therefore, taking into account the fact that the error decreases with both the increased size of the system and the basis set, we estimate that, in the coronene-circumcoronene dimer, the error of replacing aug-cc-pVTZ by the aTZ basis set ought to be smaller than 0.5%. The modification of the basis set resolves the linear dependency problem for smaller systems. However, it is not sufficient for the severe linear dependency encountered in the coronene-circumcoronene dimer. Using 64-bit precision, it was not possible to obtain results in the full basis set and it became necessary to delete from the basis set linear combinations of functions corresponding to the lowest eigenvalues of the AO overlap matrix. This method, although widely used, is not ideal, as it changes the results, and in the worst case can lead to artificial steps on the potential energy surface (PES). The aXZ basis sets do not suffer from this deficiency in smaller systems, as the elimination of redundant basis functions is performed by appropriate basis set design (see [52] for full discussion). Unfortunately, for systems larger than the coronene dimer, the aTZ basis set basis is still nearly linearly dependent, and some linear combinations of the basis functions had to be deleted. The size of aDZ basis set for the circumcoronene dimer is 2,178 contracted basis functions, while the full basis set has 2,664 functions. For the triple-zeta basis set, the numbers are 4,608 and 5,472, respectively. Even the smallest basis set (aDZ) requires removing 6 linearly dependent basis functions at the default threshold 10^{-6}. The full aug-cc-pVTZ basis set requires removing 175 basis functions using the same threshold.

We have focused on two geometries with parallel rings: sandwich and parallel displaced (PD). For the aromatic systems of this size the T-shaped geometry, which is nearly isoenergetic with the PD form in benzene, is not energetically favorable and is of lesser interest because it cannot model graphitic interactions. The intermolecular geometry optimization was performed through a series of SCS-MP2 calculations [28] in the aDZ basis set, as in our previous work on the coronene dimer [52]. There are two parallel displaced geometries, depending on whether the displacement is perpendicular to a C–C bond in the central six ring (conformer A) or parallel to it (conformer B). Just like in benzene [16] and in the coronene dimer [52], B is more stable.

The largest system treated here is the coronene-circumcoronene sandwich. We were able to perform a single QCISD(T) calculation in the 6–31G*(0.25) basis set which is a modified 6–31G* basis where the exponent of the carbon's d orbitals is set to 0.25 [56]. The purpose of this calculation was to assess whether the trends observed in our earlier calculations hold for these much larger aromatic systems. SCS-MP2 agrees very well with higher-level QCISD(T) calculations for the benzene dimer but overestimates the correlation energy, compared to QCISD(T) for the coronene dimer. The sandwich geometry was chosen because it is still feasible to perform QCISD(T) calculations due to symmetry, and the role of dispersion is larger than in the parallel displaced (PD) geometry. This is probably the largest QCISD(T) or CCSD(T) calculation, in terms of the formal scaling parameter n^3N^4 ($n = 342$ is the number of correlated electrons, and $N = 1{,}152$ is the number of basis functions) performed to date.

3 Results and discussion

Figure 1 shows the potential curves in the vicinity of the van der Waals minimum for the coronene-circumcoronene (Cor-Circ, $C_{24}H_{12}$–$C_{54}H_{18}$) heterodimer and for the circumcoronene dimer (Circ–Circ, $C_{108}H_{36}$) at the spin-component scaled MP2 (SCS-MP2/aDZ) level, for parallel displaced (PD) geometries at the optimized horizontal displacement. We also included the coronene–coronene potential curve from Ref. [52]. We have scanned the potential surfaces in the horizontal (x,y) direction. Figure 2a is a representative plot for the circumcoronene dimer, showing the characteristic corrugation of the surface on a 6.4 Å × 6.4 Å grid. This is qualitatively similar to the corresponding plot for the coronene dimer [52] but the corrugation is much more pronounced, in agreement with the larger contact area and the stronger bond. Figure 2b contains a smaller section of the surface with one global minimum and the lowest energy saddle point.

Counterpoise-corrected binding energies and geometries at the SCS-MP2/aDZ level for the sandwich and PD forms are shown in Table 1. The SCS-MP2 optimum geometries show the expected trend: with the increase in the size of a polycondensed aromatic hydrocarbon, the interaction energy increases and the interplane distance shortens. Interestingly, the interplane distance is significantly shorter for the coronene-circumcoronene (Cor-Circ) sandwich than for the circumcoronene dimer (Circ–Circ). This appears to

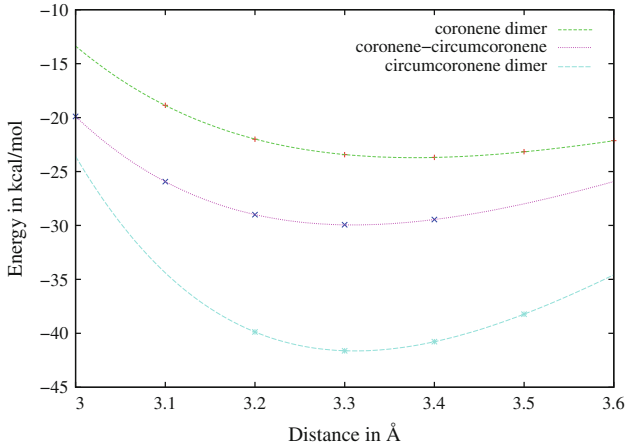

Fig. 1 Potential energy curves for the parallel displaced dimers (coronene dimer, coronene-circumcoronene dimer, and circumcoronene dimer) at the SCS-MP2/aDZ level. The *horizontal* (*X*) displacement was optimized. Energies in kcal/mol. The circumcoronene dimer curve was shifted upwards by 30 kcal/mol, the coronene-circumcoronene curve by 10 kcal/mol, while coronene dimer curve was left at its original value

be an edge effect which is absent in the heterodimer Cor-Circ. Indeed, extrapolating the Cor–Cor and Circ–Circ interplane distances as a linear function in $1/n$ to $n = \infty$, ($n = 2$ for Cor, $n = 3$ for Circ) yields almost exactly the distance for Cor-Circ which ought to be close to the value of the infinite plane. The effect is not observed in the parallel displaced configuration, probably because it has coronene carbon atoms in an edge position. However, the optimum horizontal displacement is much shorter. The cause is probably similar, the central alignment of the coronene molecule results in weaker edge effect and a stronger interaction.

Comparison of the SCS-MP2 values with experiment for the coronene-circumcoronene system, which is probably the best model for the interaction between larger graphene sheets, shows that the SCS-MP2 method overestimates the dispersion attraction and gives interplane distances which are too short. The common form of graphite has a PD configuration and a distance between layers of 3.355 Å at room temperature, decreasing to 3.337 Å at 4.2 K [57]; the room-temperature data have been confirmed by more recent high-accuracy diffraction measurements [58, 59]. Comparison with the data in Table 1 shows that the SCS-MP2 method, which virtually agrees with high-level CCSD(T) for the benzene dimer [16, 21], overbinds for these larger graphenes, a conclusion in agreement with the data on the coronene dimer [52]. The calculated equilibrium separation of planes for coronene-circumcoronene and for the circumcoronene dimer is about 1.31 Å, shorter than the r_0 zero-point distance in graphite. Because of the anharmonic nature of the potential energy surface, the

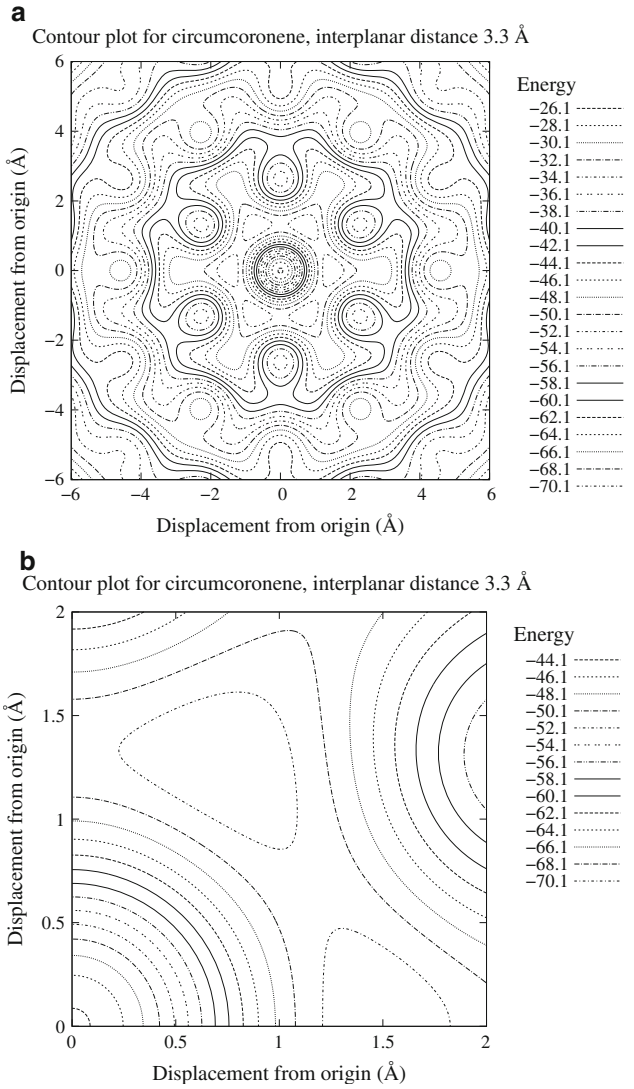

Fig. 2 A contour plot for the counterpoise-corrected SCS-MP2/aDZ interaction energy of circumcoronene dimer at a fixed interplane distance of 3.3 Å, the rings are constrained to be parallel. **a** The full potential energy surface in the (x, y) plane at 0.2 Å resolution, **b** a section near the minimum and the saddle point. (x, y) distances in Å units

experimental r_e distance is most likely less than the zero-point value (3.337 Å); we estimate it to be around 3.32 Å. (Note that most calculated values are compared uncritically with the room-temperature interlayer distance in graphite, 3.35 Å which is definitely too large for r_e).

Table 2 shows results for larger basis sets, and the effect of high-level (QCISD(T)) calculation for the coronene-circumcoronene sandwich configuration. Because of the high cost of the triples-corrected calculations, we could afford only the small 6–31G($d = 0.25$) basis set [56] that was specifically developed for economical calculations of van der Waals interactions, and only at the symmetrical sandwich geometry. Our best estimate for the binding

Table 1 SCS-MP2/aDZ binding energies (kcal/mol) and geometry parameters (Å) for parallel displaced (PD) and sandwich configurations of the coronene, coronene-circumcoronene, and circumcoronene dimers

Property	Cor-Cor[a]		Cor-Circ		Circ–Circ	
	PD	Sandwich	PD	Sandwich	PD	Sandwich
Binding energy	23.72	17.74	39.95	35.81	71.64	54.98
Layer separation	3.376	3.661	3.310	3.420	3.311	3.578
Displacement (X)	1.524	0.000	1.225	0.000	1.513	0.000
QCISD(T) binding energy	17.31	12.78				

[a] Ref. [52]

Table 2 Binding energies at various levels of theory for the sandwich configuration of the coronene-circumcoronene dimer, at the SCS-MP2 geometry (see Table 1)

Basis set	SCF	MP2	SCS-MP2	QCISD	QCISD(T)
6–31G ($d = 0.25$)	−26.38	45.53	29.57	11.82	20.29
aDZ	−24.87	53.07	35.81		
aTZ	−25.05	56.17	38.32		

energy of coronene on circumcoronene is obtained by assuming the additivity of various remaining contributions. This assumption can be checked for smaller systems, like for the coronene dimer where one could perform larger calculations. The additivity of the CCSD(T) correction was established by Sinnocrot and Sherrill [13–15]. Here we face the problem to deduce this correction for the PD configuration from the sandwich value. In the coronene dimer case, this correction is nearly proportional to the SCS-MP2 binding energy value. For instance, denoting the binding energy by BE, the QCISD(T) correction, i.e., $[BE_{QCISD(T)} - BE_{SCS\text{-}MP2}]/BE_{SCS\text{-}MP2}$ is within 1% for the parallel displaced and sandwich configurations in the coronene dimer (−24.6 and −25.5%, respectively [52]). Physically, this proportionality is quite natural if one considers triple and quadruple substitutions as double substitutions arising from a doubly excited configuration, and it has been utilized in a number of empirical scaling procedures, for instance Ref. [60]. Scaling the sandwich ΔQCI energy (−9.28 kcal/mol) in the coronene-circumcoronene system by the SCS-MP2 binding energies we obtain for the PD conformer ΔQCI = −10.35 kcal/mol, giving an estimated QCISD(T)/aDZ binding energy of 29.6 kcal/mol. Adding to this the ΔSCS-MP2 correction for basis set extension to aTZ quality, our estimate for the coronene-circumcoronene binding energy is 32.1 kcal/mol at the QCISD(T)/aTZ level.

The binding energy of coronene on graphite surface should be higher than 32.1 kcal/mol because of basis set effects beyond the triple-zeta level, geometry reoptimization, and contributions from the second end lower layers. Based on data in the benzene dimer [21], we estimate that extrapolating to a complete basis set would contribute another 0.6 kcal/mol to the binding energy. The geometry reoptimization contribution is expected to be small. The effect of multiple layers can be estimated by noting that the leading term in the effective dispersion energy (in the case of isotropic dispersion) between a molecule and an infinite plane should have a power law of R^{-4}; the change from the usual R^{-6} power law for isolated molecules is a purely geometrical effect. The effect of lower layers on the desorption energy can be thus estimated as $D(2^{-4} + 3^{-4} + 4^{-4}) = 0.082D$ where D is the dispersion energy between coronene and a single graphene layer. The latter can be estimated from Table 2 as the difference between the QCISD(T) and SCF energies, about 57 kcal/mol for the sandwich structure. Adding all contributions gives 37.4 kcal/mol for the equilibrium (D_e) adsorption energy of coronene on graphite at 0 K. The difference between the zero-point energy levels, D_0, should be somewhat lower. Depending on the method of analysis, thermal desorption experiments [61] give 1.3 ± 0.2 (30 ± 5 kcal/mol) or 1.5 ± 0.1 eV (34.6 ± 2 kcal/mol), somewhat less than our estimate. If the contribution of the hydrogens to dispersion is neglected, our best estimate for the exfoliation energy of graphite is 1.56 kcal/mol per C atom (67.5 meV). We disagree with the authors of Ref. [61] concerning the correction for the hydrogens. In an infinite graphene sheet, the C–H bonds are replaced by one half of a C–C σ bond. The dispersion interaction of the latter should be similar, and probably even slightly larger than the dispersion attraction of the C–H bond, and therefore we do not think that the coronene values should be corrected for the hydrogens. Our value is higher than the experimental estimates of 54 or 62 meV per C atom, obtained in [61] *without* performing the hydrogen

Table 3 Energies (relative to infinite separation) and geometry parameters for the minima and transition state on the horizontal (*X*, *Y*) potential surface (in kcal/mol and Å)

Property	Cor-Cor[a]		Cor-Circ		Circ–Circ	
	Minimum	Transition state	Minimum	Transition state	Minimum	Transition state
Energy	−23.72	−23.24	−39.95	−39.48	−71.64	−69.78
Layer separation	3.376	3.400	3.310	3.325	3.311	3.337
Displacement (*X*)	1.524	0.000	1.225	0.000	1.513	0.000
Displacement (*Y*)	0.000	1.405	0.000	1.096	0.000	1.331

[a] Ref. [52]

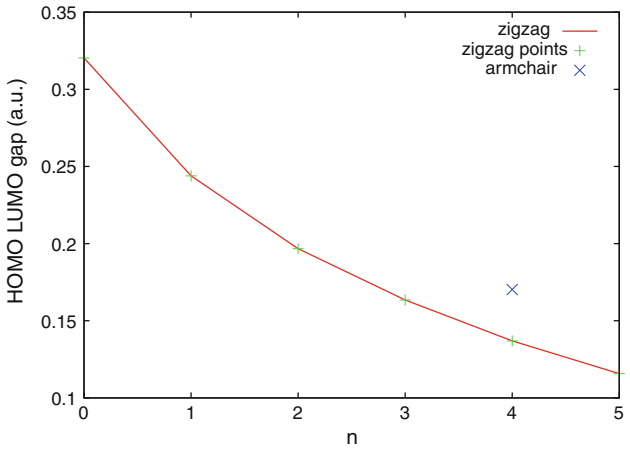

Fig. 3 The Hartree–Fock HOMO-LUMO gap for a series of circumcoronenes, $C_{24}H_{12}$ ($n = 0$) to $C_{294}H_{42}$ ($n = 5$). The single point at $n = 4$ belongs to $C_{222}H_{42}$, a graphene that is similar to $C_{216}H_{36}$ but has been reshaped to change all zigzag sides to armchair sides

correction. It is much higher than the 48 meV obtained by Langreth et al. [62] using the van der Waals density functional, and also higher than the value of Galli et al. [63], 56 meV/C, obtained from a quantum Monte Carlo calculation. Like all density functional methods, the van der Waals functional contains assumptions that cannot be tested internally, only by comparison with experiment or higher-level theory. Both calculations [62, 63], but particularly Ref. [62], predict interlayer separations which are too long (3.6 and 3.43 Å, respectively). The large interlayer separation obtained by the van der Waals density functional is in accord with the low binding energy. We will return to this problem in a future paper.

The horizontal sections of the intermolecular potential surface allow the determination of the barrier to sliding one graphene layer over the surface of another. As in the coronene dimer, this barrier is much smaller than the straight path through the sandwich geometry which has a high barrier, over 4 kcal/mol for the Cor-Circ system. The Cor-Circ data are the most representative for larger graphene sheets because edge effects are less important. The reaction path goes through the higher energy (A) parallel displaced geometry which is a first-order saddle point, in a snaking motion. Table 3 compares the energies and geometries of the minimum (PD B form) and saddle point (PD A form) for coronene on circumcoronene, and for the circumcoronene dimer. The barrier is 0.45 kcal/mol for the coronene-circumcoronene case, close to the value in the coronene dimer (0.48 kcal/mol, [52] and is surprisingly high, 1.85 kcal/mol for the circumcoronene dimer. Figure 2b shows the relevant part of the potential energy surface for the circumcoronene dimer, with minima at about (1.5, 0) and (0.75, 1.3) Å, and saddle points (transition states) at (0, 1.3) and (0.65, 1.1) Å. Although the value for coronene sliding on supercoronene is close to kT at room temperature, it is clear that larger graphenes cannot easily glide over each other. The common textbook picture explaining the lubricating properties of graphite by sliding of π systems over each other is definitely incorrect.

Our main conclusion concerning the computational method is that the SCS-MP2 method, which performs very well for smaller aromatic systems like the benzene dimer, becomes increasingly inaccurate and overestimates the dispersion energy as the graphene size increases. This is expected, as band gap (the HOMO-LUMO distance) becomes zero in the infinite graphene sheet. Figure 3 shows the Hartree–Fock HOMO-LUMO gap as a function of n for n-circumcoronene, from $n = 0$ (coronene, $C_{24}H_{12}$) through $n = 1$ (circumcoronene, $C_{54}H_{18}$) to $n = 5$ ($C_{294}H_{42}$). Also shown a molecule that is similar to 4-circumcoronene ($C_{216}H_{36}$) but the zigzag edges has been replaced by "armchair" edges; bandgaps are higher in systems without zigzag edges. With decreasing gap, the MP2 and SCS-MP2 energies are strongly overestimated. Note that a similar effect will ultimately affect the calculation of the perturbative (T) contributions. A comparison of the QCISD(T) calculation for the coronene-circumcoronene dimer (Table 2) shows the MP2 binding energy is 2.24 times larger than its QCISD(T) counterpart. The SCS-MP2 method also overestimates the π–π interaction more than in smaller rings, e.g., for this system, the SCS-MP2 binding energy is 46% larger than the QCISD(T) result. For the sandwich geometry of the coronene dimer, the

corresponding figure was 37%. It is expected that this discrepancy will further increase for larger systems.

Table 2 also indicates that the 6–31G*($d = 0.25$) basis set provides a reasonably good approximation of the energies obtained with larger basis sets. At the MP2 level, we obtain 86% of the total interaction energy of the aDZ basis set and 81% of the energy of the aTZ basis set. The difference between the aDZ and aTZ basis set is modest (aDZ yields 94.5% of the binding energy of the bigger aTZ basis). This suggests that it is more important to provide diffuse basis functions than high angular momentum polarization functions for the description of intermolecular interactions [56, 64]. In spite of its small size, the 6–31G*($d = 0.25$) basis captures the essential part of the aromatic interaction.

We have fitted the coronene-circumcoronene potential energy surface by a model potential, to identify the principal components of the interaction energy. The simplest model assumes that the long-range interactions are due to isotropic dispersion which decays as c/r^{2a}; this is a generalization of long-range dispersion, for which $a = 3$. Integrating over the circumcoronene molecule treated as a uniformly charged disk, the dispersion potential at a point on the C_6 axis is

$$V_{\text{disp}} = c\pi\left[(R^2 - s^2)^{1-a} - (R^2)^{1-a}\right]/(1-a) \qquad (1)$$

where R is the distance of the point from the ring, s is the radius of the circumcoronene molecule, treated as a fitting parameter, and c characterizes the strength of the interaction (c is negative for attraction). For $s \to \infty$ and $a = 3$ (i.e., an R^{-6} attraction), this gives the expected R^{-4} law. By fitting this formula to the SCS-MP2 energies of the circumcoronene-coronene dimer for ring separation R values in the 4.5–7.5 Å, we obtain the plausible values $a = 3.07$ (corresponding to an $R^{-6.14}$ potential) and $s = 4.55$ Å, with an RMS deviation of only 0.1 kcal/mol. This shows that the long-range interaction is essentially pure dispersion.

This model does not intend to describe the corrugated potential energy surface for the horizontal (X,Y) motion of the two molecules. A simple Lennard–Jones potential between each pair of carbon atoms, $V = -c_1 r^{-6} + c_2 r^{-12}$ gives a poor fit, both qualitatively and quantitatively, to the potential energy surface, probably because the repulsive part of the potential is not well described by atomic contributions. There is some evidence that the peripheral carbons in larger graphenes are more negatively charged than the inner carbons [8]. Using different parameters for the peripheral and inside carbon atoms give some improvement but the RMS deviation is still 1.9 kcal/mol, and the qualitatively most characteristic feature of the (X,Y) surface, the corrugation of the surface, is almost completely missing. The DFT-CC method of Bludsky et al. [65] is a promising alternative to fully empirical fittings because the difficult Pauli repulsion component is presumably well described by low-cost DFT calculations.

Acknowledgments This work was supported by the U. S. National Science Foundation under grant number CHE-0911541 and by the Mildred B. Cooper Chair at the University of Arkansas. We thank the staff of the University of Arkansas razor supercomputer for technical assistance. Acquisition of the Razor supercomputer was supported in part by the National Science Foundation under award number MRI-0959124.

References

1. Watson JD, Crick FHC (1953) Nature 171:737
2. Lerman LS (1961) J Mol Biol 3:18
3. Burley SK, Petsko GA (1985) Science 229:23
4. Hunter CA, Singh J, Thornton JM (1991) J Mol Biol 218:837
5. McGaughey GB, Gagne M, Rappe AK (1998) J Biol Chem 273:15458
6. Emseis P, Failes TW, Hibbs DE, Leverett P, Williams PA (2004) Polyhedron 23:1749
7. Lu W, Chan MCW, Zhu N, Che CM, Li C, Hui Z (2004) J Am Chem Soc 126:7639
8. Jaffe RL, Smith GD (1996) J Chem Phys 105:2780
9. Hobza P, Selzle HL, Schlag EW (1996) J Chem Phys 100:18790
10. Špirko Engvist, Soldán P, Selzle HL, Schlag EW, Hobza P (1999) J Chem Phys 111:572
11. Tzuzuki S, Lüthi HP (2001) J Chem Phys 114:3949
12. Tzuzuki S, Honda K, Uchimaru T, Mikami M, Tanabe K (2002) J Am Chem Soc 124:104
13. Sinnocrot MO, Valeev EF, Sherrill CD (2002) J Am Chem Soc 124:10887
14. Sinnocrot MO, Sherrill CD (2003) J Phys Chem A 107:8377
15. Sinnocrot MO, Sherrill CD (2004) J Phys Chem A 108:10200
16. Hill JG, Platts JA, Werner HJ (2006) Phys Chem Chem Phys 8:4072
17. Sinnocrot MO, Sherrill CD (2006) J Chem Phys 110:10656
18. Lee EC, Kim D, Jurečka P, Tarakeshwar P, Hobza P, Kim KS (2007) J Phys Chem A 111:3446
19. DiStasio RA Jr, von Helden G, Steele RP, Head-Gordon M (2007) Chem Phys Lett 437:277
20. Podeszwa R, Bukowski R, Szalewicz K (2006) J Phys Chem A 110:10345
21. Janowski T, Pulay P (2007) Chem Phys Lett 447:27
22. Kristyán S, Pulay P (1994) Chem Phys Lett 229:175
23. Slater JC (1974) Quantum theory of molecules and solids, vol 4. McGraw-Hill, New York
24. Vosko SH, Wilk L, Nusair M (1980) Can J Phys 58:1200
25. Perez-Jorda JM, Becke AD (1995) Chem Phys Lett 233:134
26. Jeziorski B, Moszynski R, Szalewicz K (1994) Chem Rev 94:1887
27. Jeziorski B, Korona T, Szalewicz K (2002) J Chem Phys 117:5124
28. Grimme S (2003) J Chem Phys 118:9095
29. Jung YS, Lochan RC, Dutoi AD, Head-Gordon M (2004) M J Chem Phys 121:9793
30. Pitonák M, Neogrády P, Černy J, Grimme S, Hobza P (2009) Chem Phys Phys Chem 10:282
31. Schwabe T, Grimme S (2008) Acc Chem Res 41:569
32. Sato T, Nakai H (2009) J Chem Phys 131:224104
33. Adamovic I, Gordon MS (2005) Mol Phys 103:379
34. Zhao Y, Truhlar DG (2006) J Chem Phys 125:194101

35. Zhao Y, Truhlar DG (2007) J Phys Chem 112:4061
36. Zhao Y, Truhlar DG (2008) Theor Chem Acc 120:215
37. Von Lilienfeld OA, Tavernelli I, Rothlisberger U, Sebastiani D (2004) Phys Rev Lett 93:153004
38. DiLabio GA (2008) Chem Phys Lett 455:348
39. Dion M, Rydberg H, Schröder E, Langreth DC, Lundqvist BI (2004) Phys Rev Lett 92:246401
40. Dion M, Rydberg H, Schröder E, Langreth DC, Lundqvist BI (2005) Phys Rev Lett 95:109902
41. Sato T, Tsuneda T, Hirao K (2007) J Chem Phys 126:234114
42. Ángyán JG, Gerber IC, Savin A, Toulouse J (2005) Phys Rev A 72:012510
43. Becke AD, Johnson ER (2007) J Chem Phys 127:154108
44. Crawford TD, Schaefer III HF (2000) In: Lipkowitz KB, Boyd DB (eds) Reviews in computational chemistry, vol 14. Wiley, New York, pp 33–136
45. Schütz M, Werner HJ (2001) J Chem Phys 114:621
46. Schütz M, Werner HJ (2000) Chem Phys Lett 318:370
47. Liakos DG, Hansen A, Neese F (2011) J Chem Theory Comput 7:76
48. Urban M, Noga J, Cole SJ, Bartlett RJ (1985) J Chem Phys 83:4041
49. Raghavachari K, Trucks GW, Pople JA, Head-Gordon M (1989) Chem Phys Lett 157:479
50. Janowski T, Ford AR, Pulay P (2007) J Chem Theory Comput 3:1368
51. Janowski T, Pulay P (2008) J Chem Theory Comput 4:1585
52. Janowski T, Ford AR, Pulay P (2010) Mol Phys 108:249
53. Pople JA, Head-Gordon M, Raghavachari K (1987) J Chem Phys 87:5968
54. Janowski T, Pulay P, Sasith Karunarathna AA, Sygula A, Saebo S (2011) Chem Phys Lett (accepted)
55. PQS version 3.3, Parallel Quantum Solutions, LLC, Fayetteville, Arkansas, http://www.pqs-chem.com
56. Van Lenthe JH, Duijneveldt-van Van, de Rijdt JGCM, van Duijneveldt FB (1987) Adv Chem Phys 69:521
57. Baskin Y, Meyer L (1955) Phys Rev 100:544
58. Trucano P, Chen R (1975) Nature 258:136
59. Howe JY, Jones LE, Ow H, Rawn CJ (2003) Powder Diffract 18:150
60. Fast PL, Corchado J, Sanchez ML, Truhlar DG (1999) J Phys Chem A 103:3139
61. Zacharia R, Ulbricht H, Hertel T (2004) Phys Rev B 69:155406
62. Chakarova-Käck S, Schröder E, Lundqvist BI, Langreth DC (2006) Phys Rev Lett 96:146107
63. Spanu L, Sorella S, Galli G (2009) Phys Rev Lett 103:196401
64. Pitonak M, Janowski T, Neogrady P, Pulay P, Hobza P (2009) J Chem Theory Comput 5:1766
65. Bludsky O, Rubes M, Soldan P, Nachtigall P (2008) J Chem Phys 128:114102